Supersymmetry-assisted high-fidelity ground-state preparation of a single neutral atom in an optical tweezer

Xi-Wang Luo,[1] Mark G. Raizen,[2] and Chuanwei Zhang[1,*]

[1]*Department of Physics, The University of Texas at Dallas, Richardson, Texas 75080-3021, USA*

[2]*Center for Nonlinear Dynamics and Department of Physics, The University of Texas at Austin, Austin, Texas 78712, USA*

(Received 7 November 2019; revised 16 November 2020; accepted 4 January 2021; published 19 January 2021)

Arrays of neutral-atom qubits in optical tweezers are a promising platform for quantum computation. Despite experimental progress, a major roadblock for realizing neutral-atom quantum computation is the qubit initialization. Here we propose that supersymmetry, a theoretical framework developed in particle physics, can be used for ultrahigh-fidelity initialization of neutral-atom qubits. We show that a single atom can be deterministically prepared in the vibrational ground state of an optical tweezer by adiabatically extracting all excited atoms to a supersymmetric auxiliary tweezer. The scheme works for both bosonic and fermionic atom qubits trapped in realistic Gaussian optical tweezers and may pave the way for realizing large-scale quantum computation, simulation, and information processing with neutral atoms.

DOI: 10.1103/PhysRevA.103.012415

I. INTRODUCTION

Neutral atoms trapped in optical tweezer arrays have emerged as a promising candidate for quantum computation and simulation [1–5] due to their attractive features such as identical qubits, large scalability through atom-by-atom assemblers [6–12], and high-precision control and measurement. For neutral-atom qubits, high-fidelity single-qubit gates have been realized using microwave or two-photon Raman transitions [13–19]. Two-qubit gates have been realized using short-range collisions or long-range Rydberg interactions [20–28], with significantly improved gate fidelity in recent years.

Significant experimental progress has been made on high-fidelity neutral-atom qubit initialization that requires deterministic preparation of a single atom in the vibrational ground state of an optical tweezer, but major obstacles still exist. For bosonic atoms, interaction blockade and single-atom rapid imaging allow the deterministic preparation of a single atom in an optical tweezer, and defect-free atom arrays with up to tens of single atoms have been demonstrated by rearranging the occupied tweezers [7–11]. However, atoms in the tweezers are subject to imaging heating and the experimental ground-state cooling is far from perfect due to photon recoil in sideband cooling [29–35]. For fermionic atoms, high-fidelity preparation of a few atoms is possible through the method of trap deformation [36–39]. However, to obtain a single-fermion ground state, the trap needs to be tilted and ramped down to an extremely low depth to spill the excess atoms, making the process very sensitive to external potential noises and requiring a long trap-deforming time to avoid heating. For both bosons and fermions, the fidelity to prepare a single atom in the ground state of a tweezer is approximately 90% [29–32,37] in realistic experiments.

Supersymmetry was first introduced within the context of particle physics and became one possible solution to many important problems in high-energy physics [40]. Though supersymmetry remains to be observed in particle physics, it has found applications in areas including condensed-matter physics, cold atoms, and optics [41–47].

In this paper we propose a supersymmetry-based scheme to achieve ultrahigh-fidelity single-atom ground-state preparation in an optical tweezer through adiabatically extracting excited atoms to its supersymmetric partner, an auxiliary tweezer. Specifically, the eigenstates of two tweezers (except the main tweezer ground state) are pairwise related to one another, yielding supersymmetry (either exact or approximate). For bosons, we can prepare a sideband-cooled single atom [29–35] and transfer its excited components to the supersymmetric auxiliary trap, followed by postselecting the measurement result with an empty auxiliary tweezer (i.e., the single atom stays in the ground state of the original tweezer). For fermions, we start from a few atoms [37] occupying the low-lying states and transfer all excited atoms to the supersymmetric auxiliary tweezer. We consider realistic Gaussian optical tweezers and show that ultrahigh-fidelity ground-state preparation can be achieved in a short time interval for both bosons and fermions. In such a qubit initialization process, supersymmetry plays an essential role for simultaneously extracting all excited components or atoms from the main tweezer to the auxiliary tweezer.

II. SUPERSYMMETRY

In quantum mechanics, supersymmetry theory involves a pair of partner Hamiltonians such that for every eigenstate $|\varphi_{1,n}\rangle$ (except the $n = 0$ ground state) of one Hamiltonian H_1, its partner Hamiltonian H_2 has a corresponding eigenstate

*chuanwei.zhang@utdallas.edu

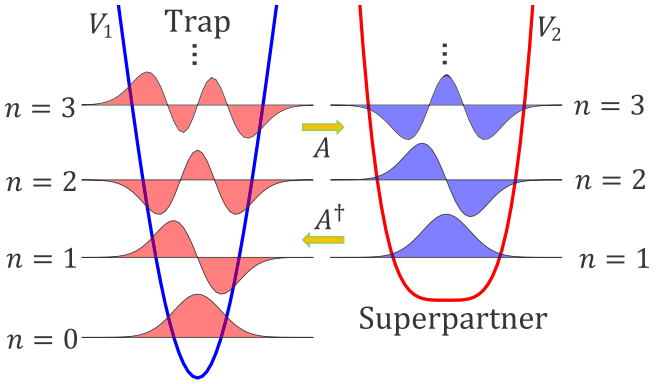

FIG. 1. Schematic illustration of a trap potential and its supersymmetric partner. Except for the ground state, all eigenvalues of the trap are exactly matched to those of its superpartner. The corresponding eigenstates are related through the action of A and $A^\dagger$.

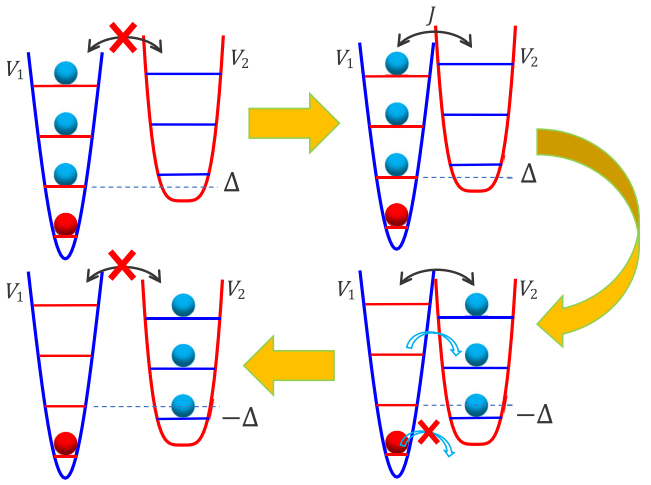

FIG. 2. Schematic illustration of adiabatic extraction of all excited atoms (or components) in the optical tweezer using the superpartner as an auxiliary tweezer. Here J and Δ are, respectively, the tunneling amplitude and detuning between two tweezers.

$|\varphi_{2,n}\rangle$ with the same energy [41]. This can be established by factorizing the Hamiltonian in terms of two operators A and $A^\dagger$,

$$H_1 = A^\dagger A, \quad H_2 = AA^\dagger, \tag{1}$$

which are isospectral with eigenstates (non-normalized) pairwise related to one another through $|\varphi_{2,n}\rangle = A|\varphi_{1,n}\rangle$ and $|\varphi_{1,n}\rangle = A^\dagger|\varphi_{2,n}\rangle$. If the ground state of H_1 is annihilated by A, i.e., $A|\varphi_{1,0}\rangle = 0$, then it does not have a corresponding state in H_2, leading to exact supersymmetry between the two Hamiltonians, as schematically illustrated in Fig. 1.

For the nonrelativistic Schrödinger problems, one can always identify two supersymmetric potentials, $V_1(x)$ and the superpartner $V_2(x)$, that are entirely isospectral except for the ground state of $V_1(x)$. Here we are interested in neutral atoms trapped in optical tweezers, and only low-energy bound states are relevant. We consider a deep optical tweezer with N_b bound states that are filled with N_a noninteracting neutral atoms ($N_\mathrm{a} \ll N_\mathrm{b}$). Only the first N bound states (with $N \ll N_\mathrm{b}$) are relevant if the system is precooled to a low temperature. Here we still call $V_2(x)$ the superpartner tweezer of $V_1(x)$ if the first N bound-state energies of $V_1(x)$ (except the ground state) are exactly matched by the first $N-1$ bound-state energies of $V_2(x)$.

III. ADIABATIC EXTRACTION

Although our scheme can be applied to any dimension, we will first limit our analysis to one spatial dimension to simplify the calculation. We assume significantly strong trapping along transverse directions, where only the ground transverse state is occupied. We consider a main optical tweezer $V_1(x)$ with noninteracting atoms populating only the first N bound states (i.e., the populations of higher-energy states are negligible) and introduce an auxiliary empty tweezer $V_2(x)$ that is the superpartner of $V_1(x)$. Within the subspace spanned by the first N bound states, the Hamiltonians read $H_1 = \sum_{n=0}^{N} E_{1,n}|\varphi_{1,n}\rangle\langle\varphi_{1,n}|$ and $H_2 = \sum_{n=1}^{N} E_{2,n}|\varphi_{2,n}\rangle\langle\varphi_{2,n}|$, with $E_{1,n} = E_{2,n}$ for $n \geqslant 1$.

The adiabatic atom extraction is performed as follows. (i) The auxiliary tweezer $V_2(x)$ is deformed such that its eigenenergies are increased by Δ. (ii) $V_2(x)$ is transported toward the main tweezer $V_1(x)$ adiabatically and the bound state $|\varphi_{1,n}\rangle$ is coupled with its counterpart $|\varphi_{2,n}\rangle$ for $n \geqslant 1$. (iii) $V_2(x)$ is adiabatically deformed to decrease its eigenenergies by -2Δ and then transported away from the main tweezer $V_1(x)$. (iv) The original empty $V_2(x)$ is restored for the next extraction. After such an adiabatic process, all atoms (or atom components) in the excited states of the main tweezer are transported to the auxiliary tweezer, while the atom (component) in the ground state $|\varphi_{1,0}\rangle$ is unaffected, as illustrated in Fig. 2. As a result, the remaining atom (component) in the main tweezer is prepared in the vibrational ground state. Here the pairwise energy levels due to supersymmetry play a central role for the atom extraction. Steps (i) and (iv) can be done very fast. We will focus on steps (ii) and (iii) in the following.

The time-dependent effective Hamiltonian can be written as $H_\mathrm{tot}(t) = H_1 + H_2 + H_\mathrm{int}(t)$ (see Appendix A), with

$$H_\mathrm{int}(t) = \sum_{n=1}^{N} \frac{\Delta_n}{2}|\varphi_{2,n}\rangle\langle\varphi_{2,n}| + J_n(t)|\varphi_{1,n}\rangle\langle\varphi_{2,n}| + \mathrm{H.c.}, \tag{2}$$

where we have neglected the far-off-resonance couplings which do not affect the adiabatic extraction. In fact, the adiabatic process is robust against perturbations, and the deformation and transport of the auxiliary tweezer are very flexible. The only requirement is that $|\Delta_n|$ and $|J_n|$ are small compared to the level splitting $|E_{1,n} - E_{1,n\pm1}|$ during the adiabatic process such that all energy levels are gapped (see Appendix B). Furthermore, even when $V_2(x)$ is not initialized as the exact superpartner of $V_1(x)$ with $E_{1,n} \neq E_{2,n}$, we can still extract all excited atoms if we have approximate supersymmetry (i.e., the symmetry breaking is weak with $|E_{1,n} - E_{2,n}| \ll |E_{1,n} - E_{1,n\pm1}|$) (see Appendix C). The extraction would fail if the supersymmetry were strongly broken.

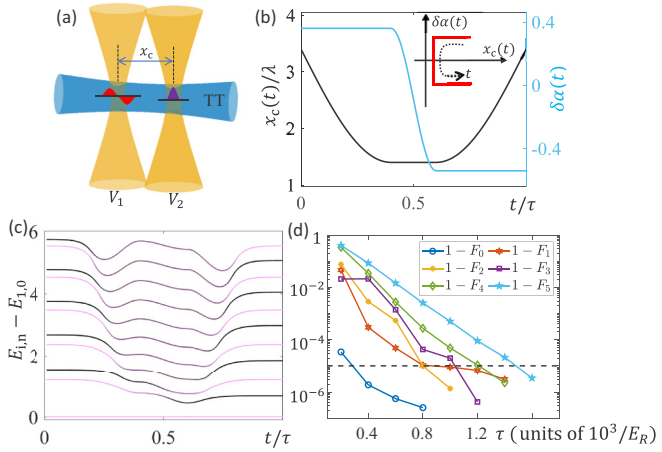

FIG. 3. (a) Gaussian optical tweezer and its superpartner with an additional transverse trap (TT). (b) Trap depth and center of the auxiliary (superpartner) tweezer as functions of time during the adiabatic extraction. The inset shows the adiabatic path. (c) Total eigenspectrum of the system along the path in (b). Colors correspond to the population probability in the two tweezers, with pink (light gray) and black representing the full population in the main and auxiliary tweezers, respectively. (d) Fidelity F_n as a function of adiabatic duration length τ.

IV. PHYSICAL REALIZATION

Although our proposal does not rely on the specific shape of the tweezer, here we consider a realistic Gaussian trap function $V_1(x) = \alpha_1 e^{-2x^2/w_0^2}$ [see Fig. 3(a)], where w_0 is the width and α_1 is the trap depth. As an example, we choose a typical width $w_0 = 1$ μm [7] and the trapping wavelength $\lambda = 810$ nm [7] and use the recoil momentum $k_R = \frac{2\pi}{\lambda}$ and energy $E_R = \frac{\hbar^2 k_R^2}{2m}$ as the units (with m the atom mass). For a deep Gaussian trap, the low-energy dynamics is approximately characterized by a harmonic oscillator with equal energy splitting. The superpartner of a harmonic trap can be easily obtained by a constant shift of the trapping potential that equals the trapping frequency. Therefore, a slight change in Gaussian trap depth leads to an approximate superpartner trap $V_2(x,t) = [\alpha_2 + \delta\alpha(t)]e^{-2[x-x_c(t)]^2/w_0^2}$. With a proper choice of α_1 and α_2 (e.g., $\alpha_1 = -12E_R$ and $\alpha_2 = -10.76E_R$), the energy levels (we consider $N = 5$ here) of two optical tweezers are paired except for the ground state of V_1 (see Appendix C). The extraction is realized by adiabatically tuning the depth $\delta\alpha(t)$ and center $x_c(t)$ of V_2, as shown in Fig. 3(b). The creation and manipulation of controlled optical tweezers can be accomplished with an electro-optic deflector which toggles between two voltages on a sufficiently fast timescale so that the atoms experience a time-averaged effective potential [48,49]. Merging and separating the supersymmetric tweezer pairs could be done by a programed sequence of voltages that is applied to an electro-optic deflector.

In Fig. 3(c) we plot the spectrum of the system during the adiabatic process along the path in Fig. 3(b), which is obtained by solving the real-space Schrödinger equation $[-\frac{\hbar^2\partial_x^2}{2m} + V_1(x,t) + V_2(x,t)]|\varphi\rangle = E|\varphi\rangle$. We see that the spectrum is gapped all the time, while the eigenstates in the two tweezers are exchanged, except for the ground state of V_1. In principle, the extraction fidelity can achieve 100% for a sufficient long adiabatic interval τ. Assuming an atom stays in state $|\varphi_{1,n}\rangle$ at time $t = 0$, we define the fidelity F_n as the probability to find the atom at time $t = \tau$ in the ground state $|\varphi_{1,0}\rangle$ of the main tweezer for $n = 0$ or in the auxiliary tweezer for $n > 0$. In Fig. 3(d) we show the fidelities as functions of τ obtained from numerically simulating the time-dependent real-space Schrödinger equation. The extraction process is a multistate Landau-Zener problem (see Appendix B), and there are couplings between different eigenstates when τ is small, yielding fidelities that are far below 1. The fidelity F_n can be close to 1 at a larger τ. For a realistic shallow trap $\alpha_1 = -12E_R$, the fidelity can be up to $F_n \gtrsim 1 - 10^{-5}$ with a short adiabatic interval $\tau \gtrsim 7$ ms ($\tau \gtrsim 70$ ms) for Li (Rb) atoms, which can be improved further by optimizing the adiabatic loop or using deeper tweezers.

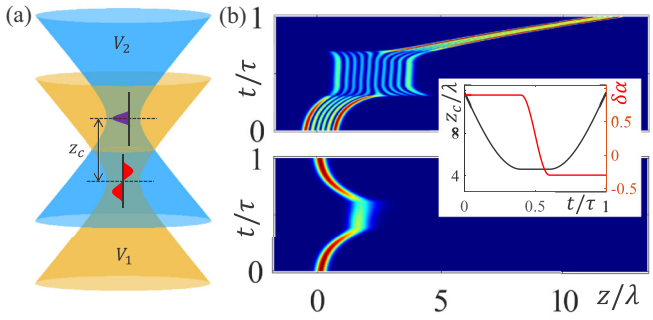

FIG. 4. (a) Two tweezers with longitudinal relative shift z_c. (b) Atom distributions during the extraction for the ground state (bottom) and the fifth excited state (top) obtained from a full 3D simulation of the Schrödinger equation. The inset shows $z_c(t)$ and $\delta\alpha(t)$ during the adiabatic process with $\alpha_1 = 200E_R$, $\alpha_2 = 198.8E_R$, and $w_0 = 0.9$ μm. The other parameters are the same as in Fig. 3. The results for the other excited state are similar. The fidelities are $F_n \sim 1$–10^{-4} (up to $n = 5$) with an adiabatic interval $\tau \sim 20$ ms ($\tau \sim 200$ ms) for Li (Rb) atoms.

We now consider the tweezer realized by a single strong and tightly focused Gaussian beam without additional transverse trapping [i.e., a three-dimensional (3D) tweezer]. The trap is given by $V_1(\mathbf{r}) = \alpha_1 \frac{w_0^2}{w_z^2} \exp[-2(x^2+y^2)/w_z^2]$, with the spot size $w_z = w_0\sqrt{1 + \frac{z^2}{z_R^2}}$ and Rayleigh range $z_R = \frac{\pi w_0^2}{\lambda}$. In this case, the tight transverse trapping, realized by the Gaussian tweezer itself, is much stronger than the longitudinal trapping. Therefore, atoms would stay in the transverse ground state with high probability after sideband cooling (laser culling) for bosons (fermions) [29,30,37], and the overall fidelity is mainly limited by the residual excitations in the longitudinal direction. We may (1) slowly bring the auxiliary tweezer to the main tweezer with their beam waists largely separated by z_c along the longitudinal direction [see Fig. 4(a)], (2) tune z_c and $\delta\alpha$ along the adiabatic path [see the inset of Fig. 4(b)], and (3) slowly move the auxiliary tweezer away from the main tweezer. Steps 1 and 3 can be done with high fidelity due to large separation of the two tweezers. Here we focus on step 2 and solve the 3D Schrödinger equation

numerically. We find that the extract fidelity can be up to $F_n \sim 1\text{–}10^{-4}$ with a proper choice of parameters, as shown in Fig. 4(b). A longer extraction time is needed to achieve higher fidelity. Here the transverse and longitudinal modes do not mix [50] for the two tweezers shown in Fig. 4(a).

V. BOSON QUBIT INITIALIZATION

We assume an initial low-temperature single-atom state (i.e., $N_a = 1$). This is because more than one atom may be left in the ground state after the extraction for $N_a > 1$ noninteracting bosons, and the energy level coupling with the auxiliary tweezer would be strongly modified for interacting bosons. Fortunately, deterministic preparation of a single boson in an optical tweezer has been realized through single-atom imaging and the atom can be further sideband cooled with a ground-state population of approximately 90% [7,29,31]. Assuming a thermal population distribution, the total probability to find the atom in $n > N$ states is less than 10^{-5} for $N = 5$. After the supersymmetric adiabatic extraction process, all excited components of the atom are transferred to the auxiliary tweezer, in which the atom number is measured. If one atom is detected in the auxiliary tweezer, we discard the atom qubit in the main tweezer and the process fails. If no atom is probed in the auxiliary tweezer, the atom must be in the ground state of the main tweezer; therefore, we keep the atom qubit in the main tweezer. The process is successful and we know with 100% probability that there is a single atom in the ground state of the main tweezer. Such postselection measurement leads to deterministic preparation of a single atom in the main tweezer with a total ground-state fidelity greater than or equal to $1 - \sum_{n>0} \frac{P_n(1-F_n)}{P_0 F_0} \geqslant 1\text{–}10^{-5}$ (P_n is the nth state occupation probability). Here postselection is to condition a probability space upon the occurrence of a given event, and the fidelity is defined as the probability to find the atom in the ground state of the main tweezer upon the occurrence of an empty auxiliary tweezer. Notice that the success probability is P_0F_0, while the probability to find an empty auxiliary tweezer is $P_0F_0 + \sum_{n>0} P_n(1 - F_n)$. Therefore, the fidelity is $P_0F_0[P_0F_0 + \sum_{n>0} P_n(1 - F_n)]^{-1} \geqslant 1 - \sum_{n>0} \frac{P_n(1-F_n)}{P_0F_0}$. The detection of the auxiliary tweezer can be done by the single-atom-resolved fluorescence imaging technique [2,15,51], where a practical issue is that the resulting scattered resonant light may be absorbed by other qubits, degrading their fidelity [note that fermions do not need resonant detection during preparation, which is an advantage (discussed below)]. The resonant scattering light could be avoided by first transferring the auxiliary-tweezer atom to another hyperfine state (e.g., $F = 2$ state of ^{87}Rb) with order of gighertz energy splitting [14], where the imaging laser (focused on the auxiliary tweezer) is far-off-resonance with the main-tweezer atoms in other qubits, and thus would not disturb their states.

VI. FERMION QUBIT INITIALIZATION

For fermions, it is more convenient to start from several atoms (e.g., $N_a = 4, 5$) distributed on the low-lying energy levels in the tweezer (see Appendix D); then we apply the supersymmetric adiabatic atom extraction process to obtain a single ground-state fermion. Note that no postselection measurement of the auxiliary tweezer is needed for fermionic qubits. We consider spin-polarized fermions with negligible interactions due to the antisymmetric wave function. The preparation fidelity is greater than or equal to $P_0 \prod_{n=0}^{N_a-1} F_n$. If one loads fermions from a reservoir with typical temperature $T/T_F = 0.5$ into a tweezer with depth $5k_BT_F$, one obtains $P_0 > 1\text{–}10^{-5}$ [52]. The total fidelity can be up to approximately $1\text{–}10^{-5}$. To obtain a tweezer with N_a low-energy atoms, one can first load a large number of fermions from a reservoir and spill excess highly excited atoms by varying the depth of the tweezer and the strength of a magnetic field gradient [36,37]. For a large N_a (e.g., $N_a = 4, 5$), the tweezer depth remains much higher than the ground-state energy whose occupation is hardly affected during the spilling process. Moreover, imperfect spilling that changes N_a by ± 1 or ± 2 does not affect our high-fidelity preparation as long as the ground state is occupied with a high probability.

It is also possible to prepare a single fermion in the ground state based on the spilling method in [36,37]; however, the overall fidelity is very limited in realistic experiments. This is because the trap needs to be tilted and ramped down to an extremely low depth, which not only makes the spilling process very sensitive to potential noises (induced by fluctuations in laser intensity and magnetic field), but also requires a long trap-deforming time to avoid heating.

VII. DISCUSSION

The fidelity might be slightly suppressed by the common heating sources existing in the system. The atom heating due to off-resonance light scattering (the rate is approximately $\frac{V}{\Delta_e}\Gamma$, with V the trap depth and Γ the damping rate of the excited state) is negligible for a large detuning Δ_e to the excited state [53]. Intensity fluctuations of the trapping lasers can be very weak and dominated by low-frequency (much smaller than the trapping frequency) noise using intensity stability techniques [54–56]; therefore, the fluctuations have very minor effects in the adiabatic process [57,58]. The fluctuation effects can be further suppressed by using the same laser source for both the main and auxiliary tweezers. The background gas collision-limited lifetime is about 10 s [7–9], which is much longer than the adiabatic duration. The adiabatic transfer times for Li and Rb atoms are about 7 and 70 ms, respectively, and both can be further improved using deeper dipole traps (the shallow trap considered above has a trapping frequency only about several kilohertz). Here the adiabatic duration can be at the same order as the sideband cooling (i.e., several milliseconds) [29]. Therefore, our scheme can lead to high fidelity and fast qubit preparation even in the presence of these common heating sources in realistic experiments. We want to point out that, for boson qubit preparation based on sideband cooling only, one could improve the fidelity by decreasing the Raman beam power and increasing the detuning with the excited state [59], but the cooling time will also increase significantly, which may enhance the heating from other sources. The cooling fidelity may also be improved using very deep traps, which is, however, quite limited for neutral atoms (typical tweezer trapping frequency ranges from several kilohertz to several tens of kilohertz, compared

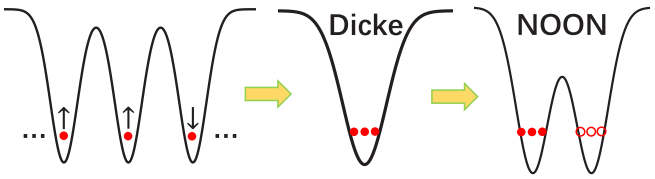

FIG. 5. Scheme to generate nonclassical entangled Dicke and NOON states by merging and splitting many single-atom tweezers. The spin states could be atomic hyperfine states.

to 10 MHz for ion traps). More importantly, our adiabatic extraction scheme applies to both fermion and boson qubit preparation, while the sideband cooling cannot be used for fermion qubit preparation with many atoms in the tweezer initially.

Combined with the capability of rearranging tweezers, our method can initialize a large array of neutral-atom (bosonic or fermionic) qubits in the vibrational ground state. In addition to quantum computation, such ground-state single-atom tweezers can be used as building blocks for generating entangled states such as Dicke and NOON states [60] that are useful for high-precision quantum metrology beyond the standard quantum limit $1/\sqrt{N}$.

The Dicke state is a symmetrized spin state with total spin J and z component m_z, corresponding to a two-mode Fock state with $J \pm m_z$ spin-up and -down atoms. Such Dicke state can be realized by merging $2J$ single-atom optical tweezers, with $J \pm m_z$ tweezers containing spin-up and -down atoms (see Fig. 5). The repulsive interaction is turned on to ensure $2J$ atoms remaining in the ground state [61] during the adiabatic evolution. Here the many-body energy gap during the adiabatic merging is roughly given by the smaller of two energy scales: the interaction energy $E_{\rm int}$ (interaction between two atoms in one tweezer) and the excited-state energy $E_{\rm e}$ (when the barriers between neighboring tweezers vanish). For typical tweezers and atom scattering lengths, $E_{\rm int}$ can be up to several tens of hertz and $E_{\rm e} \sim \frac{E_R}{4J^2}$ is around 100 Hz for $J = 10$ (i.e., 20 atoms), leading to the adiabatic merging time of approximately 10 ms.

With $2J$ atoms in the ground state of one tweezer, we can slowly switch the repulsive interaction to attractive and then split the tweezer into two identical tweezers (see Fig. 5), generating a NOON state (i.e., a coherent superposition of all particles in the left or right tweezer) [61]. If the interaction energy is smaller than the single-tweezer trapping frequency, even a sudden switching of the interaction would not excite the system [61], which is still satisfied with 20 atoms in one tweezer. During this splitting, the many-body gap is enhanced by J times compared to the merging process, and thus can be done much faster. Both Dicke and NOON states can yield measurement precision scaling as the Heisenberg limit approximately equal to $1/N$ [60].

Finally, the ability of generating a few-atom Fock state in the tweezer provides a different platform for studying few-body physics with the fixed atom number. For instance, by tuning the interaction through Feshbach resonance, it is possible to study the universality of the Efimov trimer and other multibody bound states [62–65].

VIII. CONCLUSION

In summary, we have proposed a method to deterministically prepare a single atom in the vibrational ground state of an optical tweezer with high fidelity, using a supersymmetric auxiliary tweezer. The supersymmetry is crucial for tweezer geometry design and plays a central role in extracting excited atoms. The scheme is built upon recent experimental progress on single-atom preparation and sideband cooling and applies to both fermionic and bosonic atom qubits. It addresses one major roadblock for realizing high-fidelity neutral-atom qubit initialization and therefore may pave the way for the experimental realization of intermediate-scale neutral-atom quantum computation and simulation. Our proposed qubit initialization can also be used to generate nonclassical quantum states which may find applications in other fields such as high-precision measurement and quantum sensors.

ACKNOWLEDGMENTS

X.-W.L. and C.Z. were supported by AFOSR (Grants No. FA9550-16-1-0387 and No. FA9550-20-1-0220), NSF (Grant No. PHY-1806227), and ARO (Grant No. W911NF-17-1-0128). Part of the work of C.Z. was performed at the Aspen Center for Physics, which is supported by National Science Foundation Grant No. PHY-1607611.

APPENDIX A: EFFECTIVE HAMILTONIAN

Here we show how the simple model of Eq. (2) can be used to describe the adiabatic process. We first consider the 1D case, in which a double-well trap $V(x,t) = V_1(x) + V_2(x,t)$ is formed by the two tweezers at time t during the adiabatic process. The low-energy local modes $|\varphi_{1,n}(t)\rangle$ of the left well (corresponding to the main tweezer) can be approximately obtained by solving a harmonic oscillator with curvature and center determined by the left trap minimum, and similarly for the right well (auxiliary tweezer) $|\varphi_{2,n}(t)\rangle$. Then the coupling reads

$$J_{n,m}(t) = \int \varphi^*_{1,n}(x,t)\left[-\frac{\hbar^2\partial_x^2}{2m} + V(x,t)\right]\varphi_{2,m}(x,t)dx. \tag{A1}$$

The integral $J_{n,m}$ is nonzero even when the wave functions $\varphi_{1,n}(x,t)$ and $\varphi_{2,m}(x,t)$ have opposite parity, since their parity-symmetry centers are different. As the two tweezers approach each other, the energy levels may also shift slightly, since the curvature of the main (auxiliary) tweezer would be modified by the auxiliary (main) tweezer. The full Hamiltonian reads $H_{\rm tot}(t) = H_1(t) + H_2(t) + H_{\rm int}(t)$, with

$$H_i(t) = \sum_{n=1}^{N} E_{1,n}(t)|\varphi_{i,n}\rangle\langle\varphi_{i,n}| \tag{A2}$$

and

$$H_{\rm int}(t) = \sum_{n=1}^{N} \frac{\Delta_n}{2}|\varphi_{2,n}\rangle\langle\varphi_{2,n}| + J_n|\varphi_{1,n}\rangle\langle\varphi_{2,n}| + \text{H.c.} \tag{A3}$$

The off-resonance coupling terms $J_{n,m}|\varphi_{1,n}\rangle\langle\varphi_{2,m}| + \text{H.c.}$ with $m \neq n$ are neglected.

The effective Hamiltonian is similar for the 3D case if we focus on the transverse ground-state subspace, which reads

$$J_{n,m}(t) = \int \varphi^*_{1,n}(\mathbf{r},t)\left[-\frac{\hbar^2\nabla^2}{2m} + V(\mathbf{r},t)\right]\varphi_{2,m}(\mathbf{r},t)dx. \tag{A4}$$

Here $\varphi_{1,n}(\mathbf{r},t)$ is the wave function of the nth longitudinal mode in the transverse ground state. Notice that $\varphi_{1,n}(\mathbf{r},t)$ and $\varphi_{2,m}(\mathbf{r},t)$ have the same transverse parity-symmetry center. They stay in the ground transverse state and have the same transverse parity, and therefore can couple with each other. The two tweezers are parallel to each other and they have the same optical axis as shown in Fig. 4(a); therefore, transverse and longitudinal modes do not mix for our system. In fact, the extraction of excited longitudinal modes is independent of the transverse state of the atoms in the main tweezer. Generally, the transverse modes are more confined, which typically have six (or more) times larger trapping frequency than the longitudinal modes. Therefore, high-fidelity transverse ground state can be obtained by sideband cooling for bosons or by spilling for fermions, with occupation only on the first N longitudinal modes.

APPENDIX B: ADIABATIC CONDITION

The simple model given by Eqs. (A2) and (A3) describes many independent two-level Landau-Zener processes. We have assumed that the detuning Δ_n and coupling J_n are small compared to the tweezer energy level splitting $\omega_n = E_{1,n+1} - E_{1,n}$, so the off-resonance couplings are neglected. The instantaneous eigenenergy levels and eigenstates of the nth Landau-Zener pair are $\varepsilon_{n,\pm} = E_{1,n} \pm \sqrt{J_n^2 + (\frac{\Delta_n}{2})^2}$ and $|\varphi_{\pm,n}\rangle$, with $H_{\rm tot}|\varphi_{\pm,n}\rangle = \varepsilon_{n,\pm}|\varphi_{\pm,n}\rangle$. The gap between the higher level of the nth pair and the lower level of the $(n+1)$th pair is $\varepsilon_{n+1,-} - \varepsilon_{n,+} = \omega_n - 2\sqrt{J_n^2 + (\frac{\Delta_n}{2})^2}$. We see that even for small Δ_n and J_n [e.g., $\sqrt{J_n^2 + (\frac{\Delta_n}{2})^2} \sim \frac{1}{4}\omega_n$], the eigenenergy levels $\varepsilon_{n,\pm}$ would move by $\frac{1}{2}$ their spacing, as shown in Fig. 3.

The adiabaticity condition of the two-level Landau-Zener process is $\frac{\langle\varphi_{+,n}|\dot{\varphi}_{-,n}\rangle}{\varepsilon_{n,+}-\varepsilon_{n,-}} \ll 1$. That is, the process duration should be long compared to the inverse of the gap, leading to the speed proportional to the gap. We emphasize that the full description of the adiabatic process is given by a multistate Landau-Zener problem by including off-resonance couplings $(J_{n,m}|\varphi_{1,n}\rangle\langle\varphi_{2,m}| + \text{H.c.})$. The adiabaticity condition becomes $\frac{\langle\varphi_{\mp,n}|\dot{\varphi}_{\pm,m}\rangle}{\varepsilon_{n,\mp}-\varepsilon_{m,\pm}} \ll 1$ and the adiabatic duration is long compared to all the eigenenergy gaps $\varepsilon_{n,+} - \varepsilon_{n,-}$ and $\varepsilon_{n+1,-} - \varepsilon_{n,+}$. Our full numerical simulation has taken into account all these effects.

Since a larger gap leads to a faster qubit preparation, we would like to use larger J_n and Δ_n during the adiabatic process. As we discussed above, J_n and Δ_n should still be small compared to ω_n to ensure that the all gaps are large enough. For example, one can use $\sqrt{J_n^2 + (\frac{\Delta_n}{2})^2} \sim \frac{1}{4}\omega_n$ such that $\varepsilon_{n,+} - \varepsilon_{n,-} \sim \varepsilon_{n+1,-} - \varepsilon_{n,+} \sim \frac{\omega_n}{2}$. Therefore, the speed is limited by ω_n. The speed can be very fast (10 or 100 ms preparation time for Li or Rb atoms, respectively) for the tweezers considered in this paper.

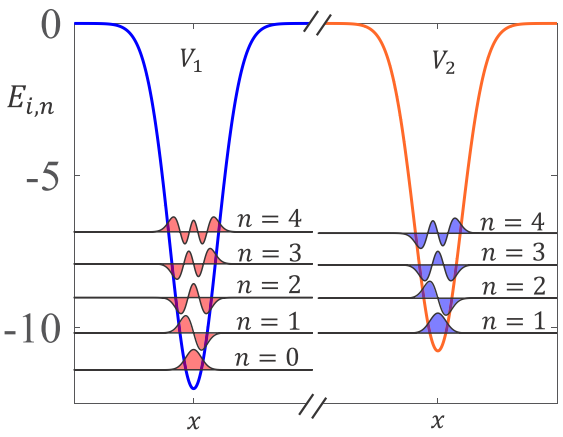

FIG. 6. Energy levels and corresponding wave functions for two Gaussian traps satisfying approximate supersymmetry with $w_0 = 1\,\mu$m, $\alpha_1 = -12E_R$, and $\alpha_2 = -10.76E_R$. The results are obtained by numerically solving the Schrödinger equation. Here E_R is the energy unit.

APPENDIX C: APPROXIMATE SUPERSYMMETRY

Exact supersymmetry requires isospectrality such that the corresponding eigenvalues of the two tweezers are exactly matched initially [i.e., $E_{1,n}(t=0) = E_{2,n}(t=0)$]. In the presence of perturbations that weakly break the energy degeneracy $E_{1,n} \neq E_{2,n}$ with $E_{1,n}(t=0) - E_{2,n}(t=0) \ll \omega_n(t=0)$, the supersymmetry becomes an approximate symmetry (an approximate symmetry arises when the symmetry is weakly broken). Our scheme works for both exact and approximate supersymmetries, i.e., in the region $E_{1,n}(t=0) - E_{2,n}(t=0) \ll \{J_n(t), \Delta_n(t)\} < \omega_n(t=0)$, such that all gaps remain during the adiabatic process. If the supersymmetry is strongly broken, we may have either unpaired states or an extremely small gap during the extraction. Therefore, the supersymmetry (either exact or approximate) is crucial for the design of our tweezer geometry and plays a central role in the atom extraction process. Two tweezer potentials that do not obey the supersymmetry would not work.

Though it is possible to obtain exact supersymmetry by tailoring the tweezer shapes, it is more realistic to work in the approximate supersymmetry region. For the 1D Gaussian example, the auxiliary tweezer corresponds to an approximate supersymmetric partner of the main tweezer (see Fig. 6). In particular, we are interested in the low-lying energy levels; therefore, the traps $V_1(x)$ and $V_2(x)$ can be approximately characterized by harmonic traps $V_1(x) \simeq \alpha_1(1 - 2x^2/w_0^2)$ and $V_2(x) \simeq \alpha_2(1 - 2x^2/w_0^2) \simeq V_1(x) + \Delta\alpha - 2\Delta\alpha x^2/w_0^2$. Besides the constant shift $\Delta\alpha \equiv (\alpha_2 - \alpha_1) \ll \alpha_1$ compared to V_1, V_2 contains an additional small term $2\Delta\alpha x^2/w_0^2$ which only leads to slight differences in the energy splittings between the two traps, i.e., $|E_{1,n} - E_{2,n}| \simeq \frac{\Delta\alpha}{\alpha_1+\alpha_2}|E_{1,n+1} - E_{1,n}|$. For a constant shift equal to the energy splitting $\Delta\alpha = E_{1,n+1} - E_{1,n}$, we obtain V_2 as the approximate superpartner of V_1 with $|E_{1,n} - E_{2,n}| \simeq \frac{1}{20}|E_{1,n+1} - E_{1,n}|$, as shown in Fig. 6. Such a tiny difference in energy splitting can be suppressed further by slightly modifying the beam waist of the auxiliary tweezer which eliminates

the curvature difference $2\Delta\alpha x^2/w_0^2$. Similar results apply to the 3D tweezers.

APPENDIX D: DIFFERENCE BETWEEN BOSON AND FERMION QUBITS

We start from the single atom (several noninteracting atoms) in the tweezer for the bosonic (fermion) qubit. In both cases (single boson or several fermions), the atom interaction is irrelevant in our ground-state preparation scheme because of the Pauli exclusion principle for fermions.

The tightly confined bosons strongly interact with each other; therefore, multioccupation is avoided as one loads the reservoir atoms into the tweezer. Through this method, defect-free single-atom tweezer arrays have been experimentally realized by postselecting and rearranging occupied tweezers [7,9,11,12]. The single atom after such a process is hot, and further sideband cooling could bring the ground-state occupation probability to approximately 90%, which means still a few excited vibrational states could be occupied. Then one can apply our supersymmetry cooling proposal to achieve ground-state preparation fidelity up to approximately 99.99%.

The case for fermionic qubits is very different because two spinless fermions do not occupy the same motional ground state and interact with each other. Therefore, the method for a bosonic qubit does not apply for a fermion qubit. A different laser culling method [36] can be used to prepare a few atoms in an optical tweezer from a reservoir of degenerate Fermi gas through gradually reducing the optical tweezer potential, as demonstrated in experiments [37]. In this case, the ground state is already occupied with a high probability and the difficulty is how to remove the last few low-lying excited-state atoms without affecting the ground-state atom. In our fermion qubit preparation, we start from a few spinless atoms distributed on the low-lying energy levels, and the supersymmetry scheme can extract all excited fermions. These spinless atoms have no interaction.

[1] N. Schlosser, G. Reymond, I. Protsenko, and P. Grangier, Sub-Poissonian loading of single atoms in a microscopic dipole trap, Nature (London) **411**, 1024 (2001).

[2] M. Saffman, T. G. Walker, and K. Mölmer, Quantum information with Rydberg atoms, Rev. Mod. Phys. **82**, 2313 (2010).

[3] I. M. Georgescu, S. Ashhab, and F. Nori, Quantum simulation, Rev. Mod. Phys. **86**, 153 (2014).

[4] D. S. Weiss and M. Saffman, Quantum computing with neutral atoms, Phys. Today **70** (7), 44 (2017).

[5] C. Gross and I. Bloch, Quantum simulations with ultracold atoms in optical lattices, Science **357**, 995 (2017).

[6] D. S. Weiss, J. Vala, A. V. Thapliyal, S. Myrgren, U. Vazirani, and K. B. Whaley, Another way to approach zero entropy for a finite system of atoms, Phys. Rev. A **70**, 040302(R) (2004).

[7] M. Endres, H. Bernien, A. Keesling, H. Levine, E. R. Anschuetz, A. Krajenbrink, C. Senko, V. Vuletic, M. Greiner, and M. D. Lukin, Atom-by-atom assembly of defect-free one-dimensional cold atom arrays, Science **354**, 1024 (2016).

[8] H. Kim, W. Lee, H. Lee, H. Jo, Y. Song, and J. Ahn, *In situ* single-atom array synthesis using dynamic holographic optical tweezers, Nat. Commun. **7**, 13317 (2016).

[9] D. Barredo, S. de Léséleuc, V. Lienhard, T. Lahaye, and A. Browaeys, An atom-by-atom assembler of defect-free arbitrary two-dimensional atomic arrays, Science **354**, 1021 (2016).

[10] W. Lee, H. Kim, and J. Ahn, Three-dimensional rearrangement of single atoms using actively controlled optical microtraps, Opt. Express **24**, 9816 (2016).

[11] D. Barredo, V. Lienhard, S. de Léséleuc, T. Lahaye, and A. Browaeys, Synthetic three-dimensional atomic structures assembled atom by atom, Nature (London) **561**, 79 (2018).

[12] D. O. de Mello, D. Schäffner, J. Werkmann, T. Preuschoff, L. Kohfahl, M. Schlosser, and G. Birkl, Defect-Free Assembly of 2D Clusters of More Than 100 Single-Atom Quantum Systems, Phys. Rev. Lett. **122**, 203601 (2019).

[13] D. D. Yavuz, P. B. Kulatunga, E. Urban, T. A. Johnson, N. Proite, T. Henage, T. G. Walker, and M. Saffman, Fast Ground State Manipulation of Neutral Atoms in Microscopic Optical Traps, Phys. Rev. Lett. **96**, 063001 (2006).

[14] C. Zhang, S. L. Rolston, and S. Das Sarma, Manipulation of single neutral atoms in optical lattices, Phys. Rev. A **74**, 042316 (2006).

[15] C. Weitenberg, M. Endres, J. F. Sherson, M. Cheneau, P. Schauß, T. Fukuhara, I. Bloch, and S. Kuhr, Single-spin addressing in an atomic Mott insulator, Nature (London) **471**, 319 (2011).

[16] D. Schrader, I. Dotsenko, M. Khudaverdyan, Y. Miroshnychenko, A. Rauschenbeutel, and D. Meschede, Neutral Atom Quantum Register, Phys. Rev. Lett. **93**, 150501 (2004).

[17] T. R. Beals, J. Vala, and K. B. Whaley, Scalability of quantum computation with addressable optical lattices, Phys. Rev. A **77**, 052309 (2008).

[18] Y. Wang, A. Kumar, T.-Y. Wu, and D. S. Weiss, Single-qubit gates based on targeted phase shifts in a 3D neutral atom array, Science **352**, 1562 (2016).

[19] C. Sheng, X. He, P. Xu, R. Guo, K. Wang, Z. Xiong, M. Liu, J. Wang, and M. Zhan, High-Fidelity Single-Qubit Gates on Neutral Atoms in a Two-Dimensional Magic-Intensity Optical Dipole Trap Array, Phys. Rev. Lett. **121**, 240501 (2018).

[20] A. M. Kaufman, B. J. Lester, M. Foss-Feig, M. L. Wall, A. M. Rey, and C. A. Regal, Entangling two transportable neutral atoms via local spin exchange, Nature (London) **527**, 208 (2015).

[21] D. Jaksch, J. I. Cirac, P. Zoller, S. L. Rolston, R. Côté, and M. D. Lukin, Fast Quantum Gates for Neutral Atoms, Phys. Rev. Lett. **85**, 2208 (2000).

[22] L. Isenhower, E. Urban, X. L. Zhang, A. T. Gill, T. Henage, T. A. Johnson, T. G. Walker, and M. Saffman, Demonstration of a Neutral Atom Controlled-NOT Quantum Gate, Phys. Rev. Lett. **104**, 010503 (2010).

[23] T. Wilk, A. Gaëtan, C. Evellin, J. Wolters, Y. Miroshnychenko, P. Grangier, and A. Browaeys, Entanglement of Two Individual

Neutral Atoms Using Rydberg Blockade, Phys. Rev. Lett. **104**, 010502 (2010).

[24] Y. Y. Jau, A. M. Hankin, T. Keating, I. H. Deutsch, and G. W. Biedermann, Entangling atomic spins with a Rydberg-dressed spin-flip blockade, Nat. Phys. **12**, 71 (2016).

[25] H. Bernien, S. Schwartz, A. Keesling, H. Levine, A. Omran, H. Pichler, S. Choi, A. S. Zibrov, M. Endres, M. Greiner, V. Vuletic, and M. D. Lukin, Probing many-body dynamics on a 51-atom quantum simulator, Nature (London) **551**, 579 (2017).

[26] H. Levine, A. Keesling, A. Omran, H. Bernien, S. Schwartz, A. S. Zibrov, M. Endres, M. Greiner, V. Vuletić, and M. D. Lukin, High-Fidelity Control and Entanglement of Rydberg-Atom Qubits, Phys. Rev. Lett. **121**, 123603 (2018).

[27] V. Lienhard, S. de Léséleuc, D. Barredo, T. Lahaye, A. Browaeys, M. Schuler, L.-P. Henry, and A. M. Läuchli, Observing the Space- and Time-Dependent Growth of Correlations in Dynamically Tuned Synthetic Ising Models with Antiferromagnetic Interactions, Phys. Rev. X **8**, 021070 (2018).

[28] T. M. Graham, M. Kwon, B. Grinkemeyer, Z. Marra, X. Jiang, M. T. Lichtman, Y. Sun, M. Ebert, and M. Saffman, Rydberg-Mediated Entanglement in a Two-Dimensional Neutral Atom Qubit Array, Phys. Rev. Lett. **123**, 230501 (2019).

[29] A. M. Kaufman, B. J. Lester, and C. A. Regal, Cooling a Single Atom in an Optical Tweezer to Its Quantum Ground State, Phys. Rev. X **2**, 041014 (2012).

[30] J. D. Thompson, T. G. Tiecke, A. S. Zibrov, V. Vuletić, and M. D. Lukin, Coherence and Raman Sideband Cooling of a Single Atom in an Optical Tweezer, Phys. Rev. Lett. **110**, 133001 (2013).

[31] Y. Yu, N. R. Hutzler, J. T. Zhang, L. R. Liu, J. D. Hood, T. Rosenband, and K.-K. Ni, Motional-ground-state cooling outside the Lamb-Dicke regime, Phys. Rev. A **97**, 063423 (2018).

[32] L. R. Liu, J. D. Hood, Y. Yu, J. T. Zhang, K. Wang, Y.-W. Lin, T. Rosenband, and K.-K. Ni, Molecular Assembly of Ground-State Cooled Single Atoms, Phys. Rev. X **9**, 021039 (2019).

[33] A. Cooper, J. P. Covey, I. S. Madjarov, S. G. Porsev, M. S. Safronova, and M. Endres, Alkaline-Earth Atoms in Optical Tweezers, Phys. Rev. X **8**, 041055 (2018).

[34] M. A. Norcia, A. W. Young, and A. M. Kaufman, Microscopic Control and Detection of Ultracold Strontium in Optical-Tweezer Arrays, Phys. Rev. X **8**, 041054 (2018).

[35] S. Saskin, J. T. Wilson, B. Grinkemeyer, and J. D. Thompson, Narrow-Line Cooling and Imaging of Ytterbium Atoms in an Optical Tweezer Array, Phys. Rev. Lett. **122**, 143002 (2019).

[36] M. G. Raizen, S.-P. Wan, C. Zhang, and Q. Niu, Ultrahigh-fidelity qubits for quantum computing, Phys. Rev. A **80**, 030302(R) (2009).

[37] F. Serwane, G. Zürn, T. Lompe, T. B. Ottenstein, A. N. Wenz, and S. Jochim, Deterministic preparation of a tunable few-fermion system, Science **332**, 336 (2011).

[38] A. N. Wenz, G. Zürn, S. Murmann, I. Brouzos, T. Lompe, and S. Jochim, From few to many: Observing the formation of a Fermi sea one atom at a time, Science **342**, 457 (2013).

[39] S. Murmann, F. Deuretzbacher, G. Zürn, J. Bjerlin, S. M. Reimann, L. Santos, T. Lompe, and S. Jochim, Antiferromagnetic Heisenberg Spin Chain of a Few Cold Atoms in a One-Dimensional Trap, Phys. Rev. Lett. **115**, 215301 (2015).

[40] M. Dine, *Supersymmetry and String Theory: Beyond the Standard Model* (Cambridge University Press, Cambridge, 2015).

[41] F. Cooper, A. Khare, and U. Sukhatme, Supersymmetry and quantum mechanics, Phys. Rep. **251**, 267 (1995).

[42] Y. Yu and K. Yang, Supersymmetry and the Goldstino-Like Mode in Bose-Fermi Mixtures, Phys. Rev. Lett. **100**, 090404 (2008).

[43] M.-A. Miri, M. Heinrich, R. El-Ganainy, and D. N. Christodoulides, Phys. Rev. Lett. **110**, 233902 (2013).

[44] M. Heinrich, M.-A. Miri, S. Stützer, R. El-Ganainy, S. Nolte, A. Szameit, and D. N. Christodoulides, Supersymmetric mode converters, Nat. Commun. **5**, 3698 (2014).

[45] B. Midya, W. Walasik, N. M. Litchinitser, and L. Feng, Supercharge optical arrays, Opt. Lett. **43**, 4927 (2018).

[46] B. Midya, H. Zhao, X. Qiao, P. Miao, W. Walasik, Z. Zhang, N. M. Litchinitser, and L. Feng, Supersymmetric microring laser arrays, Photon. Res. **7**, 363 (2019).

[47] M. P. Hokmabadi, N. S. Nye, R. El-Ganainy, D. N. Christodoulides, and M. Khajavikhan, Supersymmetric laser arrays, Science **363**, 623 (2019).

[48] V. Milner, J. L. Hanssen, W. C. Campbell, and M. G. Raizen, Optical Billiards for Atoms, Phys. Rev. Lett. **86**, 1514 (2001).

[49] N. Friedman, A. Kaplan, D. Carasso, and N. Davidson, Observation of Chaotic and Regular Dynamics in Atom-Optics Billiards, Phys. Rev. Lett. **86**, 1518 (2001).

[50] M. Schulz, H. Crepaz, F. Schmidt-Kaler, J. Eschner, and R. Blatt, Transfer of trapped atoms between two optical tweezer potentials, J. Mod. Opt. **54**, 1619 (2007).

[51] J. F. Sherson, C. Weitenberg, M. Endres, M. Cheneau, I. Bloch, and S. Kuhr, Single-atom-resolved fluorescence imaging of an atomic Mott insulator, Nature (London) **467**, 68 (2010).

[52] L. Viverit, S. Giorgini, L. P. Pitaevskii, and S. Stringari, Adiabatic compression of a trapped Fermi gas, Phys. Rev. A **63**, 033603 (2001).

[53] R. Grimm, M. Weidemüller, and Y. B. Ovchinnikov, Optical dipole traps for neutral atoms, Adv. At. Mol. Opt. Phys. **42**, 95 (2000).

[54] P. Kwee, B. Willke, and K. Danzmann, Shot-noise-limited laser power stabilization with a high-power photodiode array, Opt. Lett. **34**, 2912 (2009).

[55] J. Junker, P. Oppermann, and B. Willke, Shot-noise-limited laser power stabilization for the AEI 10 m prototype interferometer, Opt. Lett. **42**, 755 (2017).

[56] H. Vahlbruch, D. Wilken, M. Mehmet, and B. Willke, Laser Power Stabilization beyond the Shot Noise Limit Using Squeezed Light, Phys. Rev. Lett. **121**, 173601 (2018).

[57] T. A. Savard, K. M. O'Hara, and J. E. Thomas, Laser-noise-induced heating in far-off resonance optical traps, Phys. Rev. A **56**, R1095(R) (1997).

[58] C.-S. Chuu and C. Zhang, Suppression of phase decoherence in a single atomic qubit, Phys. Rev. A **80**, 032307 (2009).

[59] C. Monroe, D. M. Meekhof, B. E. King, S. R. Jefferts, W. M. Itano, D. J. Wineland, and P. Gould, Resolved-Sideband Raman Cooling of a Bound Atom to the 3D Zero-Point Energy, Phys. Rev. Lett. **75**, 4011 (1995).

[60] L. Pezzè, A. Smerzi, M. K. Oberthaler, R. Schmied, and P. Treutlein, Quantum metrology with nonclassical states of atomic ensembles, Rev. Mod. Phys. **90**, 035005 (2018).

[61] A. M. Dudarev, R. B. Diener, B. Wu, M. G. Raizen, and Q. Niu, Entanglement Generation and Multiparticle Interferometry with Neutral Atoms, Phys. Rev. Lett. **91**, 010402 (2003).

[62] S. E. Pollack, D. Dries, and R. G. Hulet, Universality in Three- and Four-Body Bound States of Ultracold Atoms, Science **326**, 1683 (2009).

[63] D. Blume, Few-body physics with ultracold atomic and molecular systems in traps, Rep. Prog. Phys. **75**, 046401 (2012).

[64] P. Naidon and S. Endo, Efimov physics: A review, Rep. Prog. Phys. **80**, 056001 (2017).

[65] C. H. Greene, P. Giannakeas, and J. Pérez-Ríos, Universal few-body physics and cluster formation, Rev. Mod. Phys. **89**, 035006 (2017).